A major purpose of the Technical Information Center is to provide the broadest dissemination possible of information contained in DOE's Research and Development Reports to business industry, the academic community, and federal, state and local governments.

Although a small portion of this report is not reproducible, it is being made available to expedite the availability of information on the research discussed herein.

1

LA-UR-83-250

Conf-830409--1

LA-UR--83-250

DE83 006074

TITLE: CHEMICAL AND TEXTURAL SURFACE FEATURES OF PYROCLASTS FROM HYDROVOLCANIC ERUPTION SEQUENCES

AUTHOR(S): Kenneth H. Wohletz

SUBMITTED TO: Workshop: Characterization and Quantification of Surface Features on Clastic and Pyroclastic Particles

MASTER

Los Alamos National Laboratory
Los Alamos, New Mexico 87545

FORM NO 836 R4
ST NO 2629 6/81

CHEMICAL AND TEXTURAL SURFACE FEATURES OF PYROCLASTS FROM HYDROVOLCANIC ERUPTION SEQUENCES

by

Kenneth H. Wohletz

Earth and Space Sciences Division
Los Alamos National Laboratory
Los Alamos, NM 87545

Manuscript received _____ ; revised _____ .

ABSTRACT

Hydrovolcanic pyroclasts are produced by the interaction of erupting magma with surface or near-surface water. Eruption energy determining pyroclast transport and depositional modes is dependent upon the amount of water interacting with magma. Grain morphologies, size distributions, surface textures, and chemical effects studied record the history of eruption cycles for volcanoes under consideration. Samples of crater-rim stratigraphic sequences from Crater Elegante and Cerro Colorado, Mexico, and from Panum Crater and Obsidian Dome, California, illustrate a basaltic tuff ring and tuff cone and two rhyolitic tuff rings respectively. Grain morphologies observed by scanning electron microscopy (SEM) reveal information on the process of melt fragmentation. Three morphologies of glass dominate particles larger than 100 μm: broken, blocky, or flat-sided grains; vesicular grains with bubble-wall textures; and drop-like grains with fluidal-form surfaces. In samples from deposits resulting from greater water interaction, particles smaller than 100 μm show increased surface area. Air-fall ashes are angular plate-like fragments; in contrast surge ashes show moss-like surfaces and agglutination of small surface particles. Transport abrasion features observed both in the field and by SEM are evidenced by overall grain rounding. Rounding is greatest for grains from planar-bed deposits, least for sandwave-bed deposits, and nearly absent on grains from fall deposits. Surface alteration and diagenesis have greater effect on pyroclasts from "wet" eruptions compared to "dry" ones. These textures are patchy overgrowths of microcrystalline and hydrated materials. Surface chemical characteristics observed with energy dispersive spectral analysis (EDS) show relative gains or losses of elements and an apparent enrichment of silica on altered surfaces.

INTRODUCTION

The scanning electron microscope (SEM) is useful in unraveling the histories of volcanic ash particles (DeRita et al., 1982; Sheridan and Marshall, 1982; Wohletz and Krinsley, 1982). Although this work is still in its infancy, the SEM has been used for over 10 years to help interpret textural features of pyroclasts (Walker and Croasdale, 1971; Heiken, 1972; Honnorez and Kirst, 1975; Huang et al., 1980). Heiken et al. (1974) and Heiken and McKay (1977, 1978) combined SEM with optical inspection of lunar materials in determining a possible pyroclastic origin. Recently, workers have attempted to develop systematics for SEM inspection of volcanic ash. Such systematics take account of the importance of bed-form variation and sample location within the outcrop, grain-size variations of samples, choice of grain type (crystal, glass, lithic), sample preparation, and the statistics of textural variations (Sheridan and Marshall, 1982).

Of great importance is the identification, geologic significance, interpretation, and origin of the multitude of textural features shown by pyroclastic particles. In the interpretation of textural origins Wohletz and Krinsley (1982) consider pyroclast histories in three developmental stages: (1) formation of major grain shape by eruption mechanism; (2) modification by transport abrasion; and (3) alteration by postemplacement processes. DeRita et al. (1982) also used this approach for analysis of crystals in pyroclastic deposits from a variety of settings.

The purpose of this paper is to examine the vertical textural variations observed in stratigraphic sections of ash and show how these can be related to the eruptive history of volcanic vents. Samples were systematically taken from near-vent localities in vertical sequences of ash layers as in Heiken and McKay (1977 and 1978). Both size distributions and petrologic (chemical)

constraints are among the features used in interpretation of textural features of the ash samples.

The samples studied in this report were taken from four small (less than 2 km diameter) volcanoes: Crater Elegante and Cerro Colorado in Sonora, and Panum Crater and Obsidian Dome, California. All four are typical volcanoes formed by hydrovolcanic eruptions. Crater Elegante is a basaltic tuff ring and Cerro Colorado is a tuff cone. The California examples are rhyolitic tuff rings. All are less than 10^5 years old. The significance of selecting these four volcanoes is that their pyroclasts have been formed by explosive mixing of meteoric water with magma as it approached the surface.

The major consideration to understand the hydrovolcanic eruptive mechanism is the energy of steam explosions. This quantity can be related to (1) the size of pyroclasts produced; (2) the mechanism of emplacement; and (3) the amount of water that interacted with the magma. The size relationship has been quantified by a standard granulometric approach (Folk and Ward, 1957), the emplacement mechanism by textural observations using the SEM, and the quantity of water by energy dispersive spectral analyses (EDS) of grain surfaces coupled with SEM observations.

Size analysis of pyroclastic materials, however, is still a controversial subject. Basic considerations are presented by Walker (1971), discussed by Sheridan (1971), and subsequent applications to hydrovolcanic materials are given by Sheridan and Updike (1975) and by Womer et al. (1980). Predictably, as hydrovolcanic eruptions increase in explosive energy, median grain size decreases, and pyroclast emplacement evolves from ballistic projection and fall into dense-laminar and lean-viscous surge (Wohletz and Sheridan, 1979). Depositional bed forms resulting from these emplacement mechanisms are respectively normally graded medium- to coarse-grained ash (pyroclastic fall);

inversely graded medium-grained planar beds (dense pyroclastic surge); massive-bedded fine- to medium-grained ash (dense-to-lean pyroclastic surge); and sandwave-bedded fine-grained ash (lean pyroclastic surge).

In this report, 20 textural descriptors (from Wohletz and Krinsley, 1982) are considered and interpreted (see Table 1). The significance of these descriptors is: (1) with decreasing water interaction during eruption, the frequency of broken, planar surfaces on pyroclasts decreases and the abundance of vesicles increases; (2) rounding and related features caused by transport abrasion increase with increasing surge density, being least for sandwave deposition (also low for fall deposition), and greatest for plane-bed deposition.

The rationale for EDS study of surface chemical trends on pyroclasts is to show the effects of posteruption diagenetic and weathering effects upon pyroclasts and also to show possible changes in magma compositions during the pyroclastic phase of a volcano. Postdepositional alteration is greatest for massive and planar surge deposits and least for sandwave beds and fall deposits. Most studies of posteruptive diagenetic or weathering effects on volcanic glass concern palagonitization (for example: Fuller, 1931; Peacock, 1926; Moore, 1966; Bonatti, 1965; Nayudu, 1964; Hay, 1960; Hay and Iijima, 1968; Jakobsson, 1978). During this process, which involves a hydration of glass, various elements are mobilized and redistributed on grain surfaces and a complex assemblage of clays and zeolite minerals develops. If ground water causes the alteration, the process is slow ($>10^3$ years), whereas if hydrothermal waters emanate from the vent, pyroclasts alter over just periods of years. A third source of water emphasized in this report is condensed steam trapped within the deposit during emplacement. Presence and quantity of this water determines whether initially fresh deposits are wet and cohesive, or dry.

The method of SEM analysis of pyroclasts is that used by Sheridan and Marshall (1982) and includes optical inspection of cleaned, sieved samples, whole grain photographs of 250-μm-sized samples and group photographs of small, less than 63-μm-sized grains. The EDS analysis used is a semi-quantitative, standardless analysis by a KEVEX 7000 series unit. Analytical precision is within one to two weight percent for silica values and within half of a percent for most other elements. At least five grains of each sample were analyzed and averaged for fresh and altered surfaces. A 15-KeV beam potential was used for analysis on relatively flat surfaces of about 200-μm^2 areas. Spot analyses of 400 μm^2 or less showed very little variation with analyses of decreasing area. The analyses of fresh grains were compared to analyses by other methods, which provided a measure of accuracy. However, the analyses reported are interpreted to show only relative variations in surface chemistry among grains and not absolute elemental abundances. These analyses are reported as oxide weight percents normalized to total 100 percent.

SAMPLE DESCRIPTION AND INTERPRETATION

Descriptive SEM features and the EDS analyses are listed in Tables 2 through 8. They illustrate the variations of pyroclast characteristics at the studied localities. Samples are from deposits which vary in median grain size from 1 cm lapilli to micron-sized ash. Size data plotted in Figure 1 show that samples fall into size fields related to bed form. Eruption energy generally increases with decreasing grain size.

Crater Elegante

Crater Elegante is in the Pinacate volcanic field, northern Sonora, Mexico (Jahns, 1959). It is a maar crater 1.6 km in diameter and 0.24 km in depth and has been studied by Gutmann (1976). The crater is surrounded by a tuff

ring with a maximum rim thickness of 50 m. The tuff ring deposit is a yellowish-tan, poorly sorted, dominantly silt- to sand-sized tephra composed of basaltic glass, crystals, and lithic materials in decreasing abundance (Table 2). The sampled rim section stratigraphy shown in Figure 2 is discussed in detail by Wohletz and Sheridan (1982) and records opening Strombolian fall eruptions, followed by Surtseyan blasts that fluctuated in energy and degree of water interaction.

Sample PIN-1 is a coarse lapilli fall of fresh gray cinder. The EDS analyses (Table 3) give an average for four grains and that of the freshest appearing grain. The analytical values are within one percent of typical values given by Gutmann and Sheridan (1978) for hawaiite basalts of that area and of Cerro Colorado basalt. This sample is a product of the opening Strombolian eruptions prior to hydrovolcanic activity. The typical vesicular shapes (Fig. 3a) with fresh surfaces were caused by fragmentation due to vesicle burst, and record little interaction with external water. Less than two weight percent of the sample exists in the fine fraction (<63 μm diameter) and these particles are characterized by blocky shapes and show few vesicle surfaces (Fig. 3b).

Sample PIN-2 marks the beginning hydrovolcanic activity and the EDS and subsequent sample analyses show significant differences from those of fresh grains (Table 3). The sample contains dominantly lithic material due to clearing of the vent during opening explosive eruptions. The blocky shape of coarse fraction grains (Fig. 3c) is typical of fragmentation due to interaction with water. The abundant, fine, micron-sized material adhered to larger fragments is evidence of origin from strong explosions. The moss-like shapes (Figure 3d) of the fine fraction grains result from high surface-area, explosive heat transfer and are another indication of the high energy of the

eruptive activity. This fraction comprises nearly 15 weight percent of the sample and would likely be much more if the small particles were not adhered to larger ones. Surface alteration is slight-to-moderate indicating that deposits were emplaced in a dry surge in which water vapor was highly superheated prior to deposition. The rounded, chipped grain edges of this sandwave deposit are the result of strong abrasion due to high-energy saltating emplacement.

PIN-3 is also from a sandwave deposit formed by a high-energy hydrovolcanic explosion. It is slightly more altered than PIN-2 and shows hydration cracks and palagonitized surfaces. Molds of crystals torn from enclosing glass are preserved (Fig. 3e) and are typical of hydrovolcanic eruptions (DeRita, et al., 1982). The fine fraction also shows the moss-like surfaces.

PIN-4 is a fine-grained ash resulting from an eruption that produced a very wet surge. The cohesiveness of the wet surge is displayed by the abundance of accretionary grains (Fig. 3f) in the coarse fraction. Twenty-five weight percent of the sample are grains less than 63 μm in diameter, however, and these tiny blocky grains show few adhering, micron-sized dust particles. Grains are totally altered to palagonite which is additional evidence for wet emplacement. These grains are rounded with relatively smooth surfaces due to abrasion that occurred during emplacement in surges.

PIN-5 is a sample of a coarse-grained planar deposit that shows both blocky grains with planar surfaces and also vesicular shapes. The alteration is moderate and only one weight percent of the deposit is in the fine fraction. This evidence suggests that PIN-5 resulted from water-poor eruptions involving expansion of magmatic volatiles. Explosive fragmentation was minimal and grains were transported in poorly-inflated surges. The grains

show many abrasion pits and surfaces that resulted from transport in a dense surge moving in laminar flow.

PIN-6, PIN-7, PIN-8 are samples of a planar, massive, and sandwave deposit respectively. This succession of deposits records a gradual increase in eruption energy. Fragmentation (percentage of fines) increases and vesiculation decreases from PIN-6 to PIN-7 and PIN-7 experienced less abrasion due to its transport in a lower density surge. Steam produced was cool enough to condense on particles evidenced by vesicle fillings of alteration material. PIN-8 is a fresh deposit showing only slight-to-moderate alteration on grains that were produced by dominantly hydrovolcanic fragmentation. Water was likely highly superheated in these energetic explosions allowing most of it to escape the surge cloud prior to condensation. Some hydration, however, is apparent in vesicles. Grains show little abrasion from transport in dilute surges.

Cerro Colorado

Cerro Colorado is a tuff cone located near Crater Elegante in the Pinacate volcanic field. It has been studied by Jahns (1959), its stratigraphy is discussed by Wohletz and Sheridan (1982), and preliminary SEM analyses are shown by DeRita et al. (1982). The steep-sided cone is built up by highly cohesive and palagonitized surge deposits which indicate much wetter eruptions than those that formed Crater Elegante. The cone encircles a crater nearly 1 km in diameter and rises over 100 m above the crater floor. The basal unit of the tuff is 10 m of thinly bedded, slightly palagonitized surges while the rest of the stratigraphic section (Fig. 4) is massive, thickly bedded, highly palagonitized tuff.

PIN-12 is a sample of a sandwave deposit near the base of the cone. This deposit is only slightly palagonitized and resulted from high-energy,

dry-surge eruptions. The blocky pyroclasts (Fig. 5a) have sharp edges rounded and smoothed by abrasion and have thin, hydrated-glass encrustations. The adhering dust on both the coarse and fine fraction reveals the strong fragmentation that occurred during eruption.

PIN-13 (Fig. 5b) illustrates a deposit resulting from wetter eruptions. Accretionary grains with strong alteration result from vapor condensing on particles, which makes them cohesive. The wetter eruptions were not as energetic, as evidenced by glass still clinging to crystals.

PIN-9 resulted from an eruption produced by vesiculation when access of water to the vent temporarily ceased. Grains show little alteration and only coarse fragmentation. The deposition by fall of this sample is evidenced by lack of edge modification by abrasion.

PIN-10 and PIN-11 are samples of massive and planar surge deposits typical of the wet eruptions that built up the cone. PIN-10 came from a more energetic surge blast than PIN-11 as shown by its finer grain size and crystals separated from glass. PIN-10 also resulted from wetter eruptions than PIN-11, as shown by its stronger hydration (Fig. 5c) and blocky and drop-like fine fraction grains (Fig. 5d). The fine fraction grains of PIN-11 are plate-like, formed by fracturing of larger grains and not by interaction with water.

Panum Crater

Panum Crater is a Holocene, rhyolite dome surrounded by a tuff ring about 500 m in diameter. It erupted on the northern end of the Mono Crater chain in east-central California (Putnam, 1938; Kistler, 1966; Wood, 1977). Initial explosive eruptions resulted from the extrusion of vesiculating rhyolite through the water-saturated alluvial deposits around Mono Lake. Both hydrovolcanic and sub-Plinian explosions occurred during formation of the tuff

ring. Late stage activity consisted of the passive extrusion of a rhyolite dome in the tuff ring crater. Samples were obtained in a pumice quarry on the southeast side of the tuff ring. The chemical analyses for the least-altered samples, PAN-2 and PAN-5, given in Table 7 are closely comparable to published analyses for Mono Crater rhyolite (Loney, 1968).

Initiation of explosive eruptions emplaced an explosion breccia over a lava flow breccia (Fig. 6). PAN-1 (Fig. 6) is a sample of a massive, surge bed within the explosion breccia. These opening explosions, as were later ones, show contributions of both magmatic vesiculation and hydrovolcanic fragmentations. Such eruptions are termed phreatoplinian by Self and Sparks (1978). This origin is characterized (Fig. 7a,b) by the vesicular but blocky nature of coarse grains, and the blocky to platy shapes of the fine fraction. The sample also contains a significant contribution of lithic material from explosions piercing the wall rock. The surge transport is indicated by smoothed edges of vesiculated blocks. Broken bubble walls are revealed by platy shapes in the fine fraction. Abundant water in the surge deposit produced moderate alteration on grains.

PAN-2 (Fig. 7c) is a sample from a sandwave deposit formed from explosions that had increased in energy over those that emplaced the earlier planar and massive surge deposits. The eruptions producing the sandwave deposit were dominantly hydrovolcanic with a minor contribution by vesiculation. High-energy transport produced abundant edge abrasion of clasts, and alteration was slight because of dry emplacement. The thin, platy forms of the fine fraction are due to fracturing along microfoliation produced in the lava as it approached the surface.

PAN-3 (Fig. 7d) is a sub-Plinian fall deposit resulting from magmatic explosion with little water interaction. Grains show no transport abrasion

and only slight alteration. The sample is from the fine-grained lower layers of this reversely graded deposit. The fine fraction only accounts for five weight percent of the sample.

Water again aided the following phreatoplinian eruptions in producing the blocky vesicular grains in the coarse sandwave deposits of PAN-4. These grains experienced significant abrasion during transport in a sandwave surge. Final eruptions were solely hydrovolcanic and produced the blocky grains shown in PAN-5 (Fig. 7e). Water interaction was limited, pyroclasts apparently were emplaced dry, and suffered no alteration by water.

Obsidian Dome

Obsidian Dome is one of the northern Inyo domes, a line of obsidian eruptions south of the Mono Crater chain in California (Wood, 1977). This glass flow varies in composition from rhyodacite to dacite. It is described by Mayo et al. (1936). The dome is surrounded by a collar of ash which forms a poorly exposed tuff ring. Samples have been obtained from a recent road cut on the western side of the dome. Explosive activity varied through stages of sub-Plinian pumice fall and hydrovolcanic explosions as water gained access to the vent. The sequence shown in (Fig. 8) demonstrates the gradual increase in hydrovolcanic activity following early magmatic, vesiculation explosions.

OBS-1 (Fig. 8) is from a coarse, pumiceous ash-fall deposit that resulted from strong vesiculation of a volatile rich magma as it reached the surface. The fine, bubble wall texture of grains is well-preserved. Grains show no abrasion features and have no alteration products on their surface (Fig. 9a).

As water grained access to the vent, eruptions became phreatoplinian. OBS-2 (Fig. 8) is a sample of a planar surge deposit. The clasts show vesicular blocky grain shapes. Vesicle edges were smoothed by surge transport. Abundant adhering dust on the fine fraction, as well as the appearance

of alteration are evidence of water interaction during eruption and emplacement.

Sample OBS-3 (Fig. 9b) shows features of increased water interaction. This sample is a vesiculated tuff (Lorenz, 1974) emplaced as a massive-bed surge. Eruptions were dominantly hydrovolcanic as the magma became depleted in volatiles. Grains are mostly nonvesicular and subrounded showing smooth surfaces from abrasion during surge transport. The wet emplacement is shown by abundant trapped steam bubbles in the deposit and moderate hydration on grain surfaces. The fine fragmentation produced by water interaction is revealed by abundant adhering dust on the fine fraction.

DISCUSSION AND CONCLUSIONS

Using SEM techniques to characterize pyroclasts is a relatively new approach. This study demonstrates a systematic interpretation of pyroclasts in vertical sequences of hydrovolcanic eruption products. The fundamental observation of grain shape allows interpretation of the relative contribution of magmatic vesiculation and hydrovolcanic water-interaction in production of pyroclasts. The energy of eruption can be inferred from the degree of transport abrasion for samples from specific bed forms in near-vent samples. For recent hydrovolcanic eruptions, the degree of surface alteration combined with the abundance of fine adhering dust allows inference for the amount of water interaction during and after deposition. EDS analyses also permit interpretation of the wetness of eruptions by showing the degree of glass alteration produced by water trapped in the deposit after emplacement.

In the samples studied, three dominant shapes of grains greater than 100 μm diameter were observed. Blocky grains with planar and curvi-planar surfaces that may cut vesicle walls are most characteristic of hydrovolcanic

fragmentation. This fragmentation mechanism appears to involve a form of brittle fracture and is likely caused by stress waves from the vapor explosions propagating through the melt. Drop-like grains with fluidal-form surfaces encasing vesicular glass were not observed as frequently as blocky forms. These shapes, however, are common in submarine volcanoes such as Surtsey. Drop-like forms suggest fluid deformation of magma fragments. Vesicular forms show surfaces whose shape is determined by bubble-wall textures (Fisher, 1963) and result from magmatic volatile explosion.

Fine fraction (<63 μm diameter) shapes also demonstrate blocky shapes. Vesicular shapes are rare. Plate-like shapes observed may represent pieces of bubble walls or fracture of brittle, foliated lava. Mossy shapes demonstrate a high surface area to diameter ratio and are common in highly explosive magma-water interactions. High surface area is a necessary condition for highly efficient, conductive heat transfer from the magma to the water.

It is clear that quantification of grain shapes would facilitate sample characterization and identification. Fourier and fractal methods (Orford and Whalley, 1982; Ehrlich and Weinberg, 1970) are an attractive means of quantification but have yet to be standardized for pyroclastics. Similarly, edge modification could be quantified. In that study, the number and types of abrasion features could be characterized. Edge modification includes the general idea of rounding as well as other kinds of abrasion features. Features that result from grain-to-grain and grain-to-substrate impacts occurring during transport were observed by Wohletz and Krinsley (1982). Abrasion is more apparent upon grains transported in dense pyroclastic surges depositing planar beds than in lean surges which deposit massive and sandwave beds. Abrasion features observed in this study include grooves or scratches, dish-shape fractures, step-like fractures, and chipped or flaked areas. The

type of abrasion feature may be due to the energy of impact. The number of impacts is a function of transport distance and spacing of grains during flow, a measure of surge or flow density (Wohletz and Krinsley, 1980). Furthermore, coarse grains show more edge modification than do the fines.

Alteration features are very complex; most common is palagonitization and hydration of glass. The source of the water of hydration and its chemical effects are still poorly understood. For hydrovolcanic deposits of recent age, Wohletz and Sheridan (1982) show evidence that most palagonitization may be due to water trapped in the deposit during pyroclast emplacement. Dry deposits (sandwave surge and ash fall) show less palagonitization because steam segregated from the pyroclasts prior to deposition. Conversely, wet deposits (massive and planar surge) show strong palagonitization because steam condensed on pyroclasts during transport and produced highly cohesive wet deposits. Dry and wet deposits have been found to be interstratified in tuff cones and tuff rings. Vents erupting in shallow marine or lake waters often show more palagonitization than those in continental areas where only ground water existed during eruption. Hence, the amount of water present in the environment during eruption affects the degree of palagonitization as well as the energy of explosions (Sheridan and Wohletz, 1981). Complexities in this relationship arise from postemplacement hydrothermal activity, surface weathering, and ground-water movement.

Alteration features observed in this study include hydration rinds and cracks, microcrystalline overgrowths and encrustations, and vesicle fillings. Furnes (1975) experimentally studied palagonitization and found that it results in a redistribution of elements in glass. The redistribution may be observed as either a gain or loss of an element from its initially fresh, unaltered abundance. The EDS analyses show the relative elemental gains and

losses and are plotted in Figure 10 for the sampled stratigraphic sections. For Crater Elegante and Cerro Colorado the major element chemistry varies considerably moving up section from the fresh, basaltic sample PIN-1 to altered samples in those two hydrovolcanic sequences. SiO_2 and Al_2O_3 exhibit the strongest apparent absolute variations, but FeO, Na_2O, and CaO abundances show the greatest relative change from their initial values. SiO_2 and Al_2O_3 show opposing losses and gains that are complexly related to bed form. Fall deposits show the least alteration. Wetness of emplacement increases in a general manner from sandwave and planar to massive beds. FeO values show the most consistent and apparent changes that can be related hydrovolcanic alteration. For rhyolite samples, alteration changes are much less pronounced because rhyolite glasses are not as reactive to water as basaltic glass (Marshall, 1961; Hawkins and Rustum, 1963). In Figure 11 adapted from Furnes (1975), the progressive loss of oxides is plotted against increasing water content of basaltic palagonite. The alkalis and iron show the greatest relative changes while silica and alumina the least as shown in Figure 10. Altered basalts of Crater Elegante and Cerro Colorado show relative changes of SiO_2 and Al_2O_3 of about 18 to 31 percent corresponding to water gains of 8 to 15 percent. FeO shows a loss of 50 to 82 percent corresponding to water gains of 10 to 20 weight percent for these samples. In this manner, surface chemical analyses by EDS allow a rough estimate of the relative degree of grain alteration. When considered with size and SEM analysis, this method can provide data on the amount of magma water interaction that has produced hydrovolcanic tephra.

In conclusion, pyroclastic material can provide useful data and information about eruptive activity. The SEM coupled with grain size data and

surface chemical analysis by EDS is an effective method for studying pyroclasts. The methods fit into current standard techniques of pyroclastic studies where samples are prepared by sieving analysis and optical microscopy identification of constituent grains. EDS systems are common companion hardware on SEM setups and with improved software techniques can provide quick, approximate analyses that allow further characterization and identification of pyroclastic material.

This study shows that grain shapes, sizes, and surface textures vary systematically. For hydrovolcanic eruption sequences, blocky and vesicular shapes reveal the relative contribution of magmatic vesiculation and magma-water interaction in formation of pyroclasts. The grain sizes of ash samples permit evaluation of the energy of explosive fragmentation. Highly explosive events result in development of abundant fine material (less than 63 μm) that adheres to larger particles. The degree of grain rounding and amount of edge modification increases with density of surge and flow deposition. The amount of postemplacement alteration increases with the wetness of emplacement, and so is a measure of the degree of water-magma interaction.

ACKNOWLEDGMENTS

Roland Hagan, Robert Raymond, and Ronald Gooley of Los Alamos National Laboratory helped in the development of the EDS techniques. Donatella DeRita of the University of Rome assisted in collection of samples from Crater Elegante and Cerro Colorado. I especially thank Aaron Waters who improved the manuscript with a thoughtful review. The work was completed while the author was on postdoctoral appointment at Los Alamos National Laboratory, which is operated by the University of California for the U.S. Department of Energy.

REFERENCES

Bonatti, E., 1965, Palagonites, hydroclastites and alteration of volcanic glass in the ocean: Bull. Volcanol., v. 28, p. 257-269.

DeRita, D., Sheridan, M. F., and Marshall, J., 1982, SEM surface textural analysis of phenocrysts from pyroclastic deposits at Baccano and Sacrofano volcanoes, Latium, Italy: in Whalley, W. B. and Krinsley, D. H., eds., Scanning Electron Microscopy in Geology, Geoabstracts, Inc., Norwich, England.

Ehrlich, R., and Weinberg, B., 1970, An exact method for characterization of grain shape: Jour. Sed. Petrol., v. 40, p. 205-212.

Fisher, R. V., 1963, Bubble-wall texture and its significance: Jour. Sed. Petrol., v. 33, p. 224-235.

Folk, R. L., and Ward, W. C., 1957, Brazos River bar, a study in the significance of grain size parameters: Jour. Sed. Petrol., v. 27, p. 3026.

Fuller, R. E., 1931, The aqueous chilling of basaltic lava on the Columbia River Plateau: Amer. Jour. Sci., v. 21, p. 281-300.

Furnes, H., 1975, Experimental palagonitization of basaltic glasses of varied composition: Contrib. Min. Petrol., v. 50, p. 105-113.

Gutmann, J. T., 1976, Geology of Crater Elegante, Sonora, Mexico: Geol. Soc. Amer. Bull., v. 87, p. 1718-1729.

Gutmann, J. T., and Sheridan, M. F., 1978, Geology of the Pinacate volcanic field: State of Arizona Bureau of Geology and Mineral Technology Special Paper No. 2, p. 47-59.

Hawkins, D. B., and Rustum, R., 1963, Experimental hydrothermal studies on rock alteration and clay mineral formation: Geochim. Cosmochim. Acta, v. 27, p. 1047-1054.

Hay, R. L., 1960, Rate of clay formation and mineral alteration in a 4000-year-old volcanic ash soil on St. Vincent, B.W.I.: Amer. J. Sci., v. 258, p. 354-368.

Hay, R. L., and Iijima, A., 1968, Nature and origin of palagonite tuffs of the Honolulu group on Oahu, Hawaii: Geol. Soc. Amer. Memoir 116, p. 331-376.

Heiken, G. H., 1972, Morphology and petrography of volcanic ashes: Geol Soc. Amer. Bull., v. 83, p. 1961-1988.

Heiken, G. H., and McKay, D. S., 1977, A model for eruption behavior of a volcanic vent in eastern Mare Serenitatis: Proc Lunar Sci. Conf. 8th, p. 3243-3255.

Heiken, G. H., and McKay, D. S., 1978, Petrology of a sequence of pyroclastic rocks from the valley of Taurus-Littrow (Apollo 17 landing site): Proc. Lunar Sci. Conf. 9th, p. 1933-1943.

Heiken, G. H., McKay, D. S., and Brown, R. W., 1974, Lunar deposits of possible pyroclastic origin: Geochim. Cosmochim. Acta, v. 88, p 1703-1718.

Honncrez, J., and Kirst, P., 1975, Submarine basaltic volcanism: morphometric parameters for discriminating hydroclastites from hydrotuffs: Bull. Volcanol., v. 34, p. 1-25.

Huang, T. C., Varner, J. R., and Wilson, L., 1980, Micropits on volcanic glass shards: laboratory simulation and possible origin: Jour. Volcanol. Geotherm. Res., v. 8, p. 59-68.

Jahns, R. H., 1959, Collapse depressions of the Pinacate volcanic field, Sonora, Mexico: Arizona Geolog. Soc. Southern Arizona Guidebook II, p. 165-184.

Jakobsson, S. P., 1978, Environmental factors controlling the palagonitization of Surtsey tephra, Iceland: Geol. Soc. Denmark Bull., v. 27, p. 91-105.

Kistler, R. W., 1966, Geological map of the Mono craters quadrangle, Mono and Tuolume counties, California: U.S. Geol. Sur., Map GQ-462.

Loney, R. H., 1968, Structure and composition of the southern coulee, Mono craters, California: Geol. Soc. Amer., Memoir 116, p. 415-440.

Lorenz, V., 1974, Vesiculated tuffs and associated features: Sedimentology, v. 21, p. 273-291.

Marshall, R. R., 1961, Devitrification of natural glass: Geol. Soc. Amer. Bull., v. 72, p. 1493-1520.

Mayo, E. B., Conant, L. C., and Chelikowsky, J. P., 1936, Southern extension of the Mono Craters, California: Amer. J. Sci., v. 32, p. 81-97.

Moore, J. G., 1966, Rate of palagonitization of submarine basalt adjacent to Hawaii: in Geological Research 1966, U.S. Geol. Sur. Prof. Paper 550-D, p. 163-171.

Nayudu, Y. R., 1964, Palagonite tuffs (hydroclastites) and the products of post-eruptive processes: Bull. Volcanol., v. 27, p. 392-410.

Orford, J. D., and Whalley, W. B., 1982, The use of the fractal dimension to characterize particle form in SEM micrographs: Workshop on Characterization and Quantification of Surface Features on Clastic and Pyroclastic Particles, Tempe, Arizona, April 1982.

Peacock, M. A., 1926, The basic tuffs: in Tyrell, G. W. and Peacock, M. A., eds., The Petrology of Iceland, Roy. Soc. Edinburgh Trans., v. 45, p. 51-76.

Putnam, W. L., 1938, The Mono craters, California: Geog. Rev., v. 28, p. 68-82.

Self, S., and Sparks, R. J. S., 1978, Characteristics of widespread pyroclastic deposits formed by the interaction of silicic magma and water: Bull. Volcanol., v. 41, p. 196-212.

Sheridan, M. F., 1971, Particle-size characteristics of pyroclastic tuffs: Jour. Geophys, Res., v. 76, p. 5627-5634.

Sheridan, M. F., and Marshall, J., 1982, SEM examination of pyroclastic materials: basic considerations: SEM Incorporated, in press.

Sheridan, M. F., and Updike, R. G., 1975, Sugarloaf Mountain tephra - a Pleistocene rhyolitic deposit of base-surge origin: Geol. Soc. Amer. Bull., v. 86, p. 571-581.

Sheridan, M. F., and Wohletz, K. H., 1981, Hydrovolcanic explosions: the systematics of -tephra equilibration: Science, v. 212, p. 1387-1389.

Walker, G. P. L., 1971, Grain-size characteristics of pyroclastic deposits: Jour. Geol., v. 79, p. 696-714.

Walker, G. P. L., and Croasdale, R., 1971, Characteristics of some basaltic pyroclastics: Bull. Volcanol., v. 35, p. 305-317

Wohletz, K. H., and Krinsley, D. H., 1980, Scanning electron microscopy of volcanic ash: Proc. Lunar Sci. Conf. 11th, p. 1263-1264.

Wohletz, K. H., and Krinsley, D. H., 1982, Scanning electron microscopy of basaltic hydromagmatic ash: in Whalley, W. B. and Krinsley, D. H., eds, Scanning Electron Microscopy in Geology, Geoabstracts, Inc., Norwich, England.

Wohletz, K. H., and Sheridan, M. F., 1979, A model of pyroclastic surge: Geol. Soc. Amer. Spec. Paper 180, p. 177-193.

Wohletz, K. H., and Sheridan, M. F., 1982, Hydrovolcanic explosions II: evolution of basaltic tuff rings and tuff cones: Am. Jour. Sci.

Womer, M. B., Greeley, R., and King, J. S., 1980, The geology of Split Butte - a maar of the south-central Snake River plain, Idaho: Bull. Volcanol., v. 43, p. 453-471.

Wood, S. H., 1977, Distribution correlation, and radiocarbon dating of late Holocene tephra, Mono and Inyo Craters, eastern California: Geol. Soc. Amer. Bull., v. 88, p. 89-95.

TABLE 1
CLASSIFICATION OF PYROCLAST MORPHOLOGY AND TEXTURE

Eruptive Mechanism (Grain Shape)	Transport (Edge Modification)	Alteration (Palagonitization)
* blocky, curvi-planar surfaces	* grain rounding	* vesicle fillings
* vesicularity	* grooves and scratches	* skin cracks
* drop-like or fused skin	* step-like fractures	* solution and precipitation
* deformation planes	* dish-shape fractures	* microcrystalline encrustation
* adhering particles	* chipped edges	
* platy	* cracks	
* moss-like	* upturned plates	
	* v-shape depressions	

TABLE 2
SEM FEATURES OF CRATER ELEGANTE SAMPLES

Sample and Bed form*	Grain Shape	Edge Modification	Alteration	Fine Fraction (weight percent)	Distinguishing Features
PIN-1 F	vesicular	none	none	broken, clean surfaces (2%)	delicate shape preserved
PIN-2 SW	blocky, planar surfaces few vesicles	rounded, large chips	slight to moderate	moss-like (15%)	abundant adhering micron-sized surface material
PIN-3 SW	blocky, planar surfaces few vesicles	rounded large chips	moderate, hydration cracks	moss-like (12%)	adhering material, but less than PIN-2
PIN-4 M	blocky, accretionary masses	rounded smooth	high, totally altered to palagonite	blocky, little adhering material (25%)	uneven surfaces of many small blocks and plates stuck together
PIN-5 P	blocky and vesicular	subangular, many small chips on edges	moderate, some fresh surfaces	broken, angular chips with fine adhering grains (1%)	abrasion features are well preserved many fracture surfaces
PIN-6 P	blocky with few vesicle surfaces	subrounded, chipped surface	moderate to high, vesicles filled with alteration material	broken, angular chips with fine adhering grains (2%)	abrasion features are well preserved many fracture surfaces
PIN-7 M	blocky and vesicular	subangular, small chips on edges	moderate vesicle fillings	blocky, abundant adhering material (13%)	alteration masking abrasion features
PIN-8 SW	blocky with few vesicles	subangular with smoothed edges	slight to moderate with some fresh surfaces	clean, blocky nonvesicular (5%)	hydration rind in vesicles

* Bed forms are: F - fall, SW - sandwave, M - measure, and P- planar.

TABLE 3
EDS ANALYSIS - ELEGANTE

	Fall PIN-1*		SW PIN-2	SW PIN-3	M PIN-4	P PIN-5	P PIN-6	M PIN-7	SW PIN-8
Na_2O	3.55	2.36	0.11	1.50	1.37	0.93	1.36	1.86	1.73
MgO	4.70	3.80	1.70	2.72	3.28	2.50	3.74	4.94	2.64
Al_2O_3	13.08	16.85	14.41	16.80	19.61	14.36	17.18	2..66	15.84
SiO_2	46.54	50.45	62.64	63.78	58.54	67.07	60.81	52.35	62.61
K_2O	3.10	2.84	2.03	2.64	3.36	2.55	3.24	3.50	1.9
CaO	6.54	8.31	6.83	5.05	5.06	4.68	3.70	5.12	6.61
TiO_2	5.07	4.26	3.29	3.67	3.46	3.28	3.50	3.58	2.36
MnO	3.56	2.21	0.06	1.11	1.60	0.44	0.89	1.37	0.62
FeO	13.86	6.70	9.37	2.93	3.67	4.21	5.50	5.62	6.01
Glass	86.0	-	22.0	88.0	89.0	80.0	87.0	89.0	67.0
X-tal	11.0	-	12.0	7.0	9.0	13.0	9.0	9.0	26.0
Lithic	3.5	-	67.0	5.0	2.0	7.0	4.0	2.0	7.0

* Analysis of freshest appearing pyroclast and average analysis of sample respectively.

TABLE 4
SEM FEATURES OF CERRO COLORADO SAMPLES

Sample and Bed form	Grain Shape	Edge Modification	Alteration	Fine Fraction (weight percent)	Distinguishing Features
PIN-12 SW	blocky, drop-like	subrounded, smoothed chipped	crusty hydration rind	blocky with abundant adhering dust (7%)	adhering dust on coarse grains
PIN-13 M	Accretionary, blocky	rounded, dish shaped fractures	high granular material covering surface	blocky cores with accreted fine dust (11%)	glass enclosing crystals, accretionary lapilli
PIN-9 P	vesicular	subangular, few chipped surfaces	few vesicle fillings, fresh surfaces	angular plates and blocks (1%)	solution pits
PIN-10 M	blocky vesicular	subrounded, grooves and chip	moderate to high granular encrustation	angular blocky and drop-like (9%)	crystal molds in glass
PIN-11 P	blocky	subrounded, grooves dish-shaped fractures	moderate hydration cracks and skin, fresh areas	plate-like (1%)	glass enclosing crystals

TABLE 5
EDS ANALYSIS - COLORADO

	Fall PIN-1	SW PIN-12	M PIN-13	Fall PIN-9	M PIN-10	P PIN-11
Na_2O	2.36	1.14	1.28	-	0.88	0.62
MgO	3.84	2.49	2.99	1.67	1.61	1.67
Al_2O_3	16.85	10.78	13.54	11.58	12.48	11.58
SiO_2	50 45	69.67	62.55	69.55	69.88	71.01
K_2O	2.84	3.02	2.78	1.95	1.68	1.58
CaO	8.31	3.64	4.92	5.45	5.24	5.27
TiO_2	4.26	2.97	3.56	2.63	2.68	2.43
MnO	2.21	1.96	1.66	-	0.83	-
FeO	6.70	4.33	6.57	8.17	5.21	5.94
Glass	86.00	87.00	86.00	92.50	88.00	82.00
X-ta	11.00	12.00	14 00	4.50	10.00	17.0
Lithi	- 50	1.00	1.00	2.00	1.50	1.00

TABLE 6
SEM FEATURES OF PANUM CRATER SAMPLES

Sample and Bed form*	Grain Shape	Edge Modification	Alteration	Fine Fraction (weight percent)	Distinguishing Features
PAN-1 R	vesicular, blocky	subangular, smooth rounded vesicle edges	moderate with vesicle fillings	blocks and plates, some adhering (9%)	vesicular with lithic material
PAN-2 SW	blocky	subangular, grooves, dish shapes fractures	slight, mostly clean surfaces	very thin plates, abundant micron-size dust (11%)	impact fractures
PAN-3 F	blocky, vesicular	angular none	slight, clean surfaces	blocks and plates, no fine dust (5%)	no abrasion
PAN-4 SW	blocky, vesicular	subrounded, stepped and dish-shape fractures	slight, vesicle fillings	blocks, adhering dust (1%)	highly abraded edges
PAN-5 P	blocky	angular, chipped edges	none	blocks, no adhering dust (2%)	clean surfaces few vesicles

TABLE 7
EDS ANALYSIS PANUM AND OBSIDIAN DOME

	R PAN-1	SW PAN-2	Fall PAN-3	SW PAN-4	P PAN-5	Fall OBS-1	P OBS-2	R OBS-3
Na_2O	1.37	1.39	1.67	1.50	1.52	1.37	0.91	0.94
MgO	1.59	1.30	1.54	1.51	1.48	1.60	0.37	0.39
Al_2O_3	13.49	12.62	12.97	12.86	13.07	14.44	17.68	16.34
SiO_2	67.72	72.45	69.39	68.45	70.83	65.56	68.58	70.02
K_2O	5.80	5.55	5.94	6.01	5.77	6.68	7.29	7.72
CaO	2.40	1.85	2.23	2.34	2.01	3.03	2.25	2.30
TiO_2	2.14	1.64	2.07	2.22	1.79	2.33	0.57	0.86
MnO	1.86	1.26	1.67	1.98	1.40	1.85	0.07	.
FeO	3.62	1.97	2.64	3.13	1.29	3.15	2.32	1.54
Glass	85.9	74.0	83.0	87.0	83.0	74.0	83.0	88.0
X-tal	4.7	24.0	12.5	8.0	12.0	19.0	15.0	9.0
Lithic	9.4	2.0	4.5	4.8	4.0	7.0	2.0	3.0

TABLE 8
SEM FEATURES OF OBSIDIAN DOME SAMPLES

Sample and Bed form	Grain Shape	Edge Modification	Alteration	Fine Fraction (weight percent)	Distinguishing Features
OBS-1 F	vesicular, sharp prong-like edges	angular, none	none	plates from broken bubble walls (2%)	delicate vesicle walls preserved
OBS-2 P	vesicular, blocky	subangular, smoothed vesicle edges	slight to moderate, vesicle fillings	plates from broken bubble walls with adhering dust (8%)	smoothed vesicle edges
OBS-3 R	blocky, few vesicles	subrounded, smoother grain edges, dish like fractures	moderate, hydrated skin	blocky and platy, abundant adhering dust (8%)	smooth planar surfaces

FIGURE CAPTIONS

Fig. 1. Size distribution of samples included in this study. Rhyolitic samples are shown by open symbols and basaltic samples are solid symbols. The rhyolitic samples are generally coarser grained which reflects compositional effects upon fragmentation mechanism.

Fig. 2. Rim stratigraphic section from Crater Elegante showing sample locations and description.

Fig. 3. Micrographs of Crater Elegante pyroclasts. (a) Sample PIN-1 showing the vesicular and fresh surfaces of the coarse fraction. (b) Blocky vesicle-poor shapes of the fine fraction of PIN-1. (c) Sample PIN-2 coarse fraction is blocky with abundant adhered dust and slight surface alteration. (d) PIN-2 fine fraction pyroclasts are high surface area, moss-like shapes. (e) Sample PIN-3 shows rounded, blocky shape with a mold of a crystal that was torn from the glass during eruption. The left view is that of secondary electrons and the right a backscattered image. The surface shows slightly more alteration than that of PIN-2. (f) Sample PIN-4 showing accretionary particles on the surface of this grain from a wet surge.

Fig. 4. Rim stratigraphic section from Cerro Colorado. The lower, thinly bedded surge deposits resulted from drier eruptions than those in the upper massive section.

Fig. 5. Micrographs of Cerro Colorado pyroclasts. (a) Sample PIN-12 shows a blocky pyroclast with adhering dust and alteration. (b) Sample PIN-13 showing a rounded accretionary grain with strong alteration that resulted from a wetter eruption than PIN-12. (c) The coarse fraction of PIN-10 illustrates the highly altered surface of grains showing hydration cracks (skin) and plucked crystal molds. (d) The fine fraction of PIN-10 shows both blocky and drop-like shapes characteristic of strong water interaction during eruption.

Fig. 6. Rim stratigraphic section at Panum Crater.

Fig. 7. Micrographs of Panum Crater pyroclasts. (a) Sample PAN-1 is from a massive bed in the basal explosion breccia. A grain from the coarse fraction shows vesicular and blocky shape with a moderate amount of alteration in vesicles. The fine fraction (b) shows blocky and platy shapes of broken vesicle walls. (c) Sample PAN-2 shows angular, blocky shape with edge modification due to transport abrasion. (d) Sample PAN-3 shows elongate, vesicular shape resulting from a magmatic eruption. (e) Sample PAN-5 shows clean, planar surfaces of a blocky grain with dish-shape fractures and grooves due to transport abrasion.

Fig. 8. Rim stratigraphic section of the tuff ring surrounding Obsidian Dome. Sampled sequence records magmatic, sub-Plinian pumice fall, planar-bedded, dry-surge, and vesiculated, massive wet-surge.

Fig. 9. Micrographs of Obsidian Dome pyroclasts. (a) Sample OBS-1 showing well-preserved, vesicular shape with fresh surfaces. (b) Sample OBS-3 showing blocky, rounded shape and moderate alteration on surfaces.

Fig. 10. Major element abundances of samples taken in stratigraphic sections. The average and sample 1 for Crater Elegante are approximations of fresh basalt for both Elegante and Cerro Colorado. The stippled lines show elemental abundances for analyses of samples taken higher in the sections reflects alteration due to palagonitization. Sample bed-form types are designated as F - fall, SW - sandwave surge, M - massive surge, and P - planar surge.

Fig. 11. Plot of relative change in oxide abundance versus weight percent water analyzed in basaltic palagonite (adapted from Furnes, 1975). Solid, vertical bars show the relative gain or loss of SiO_2 for three degrees of hydration.

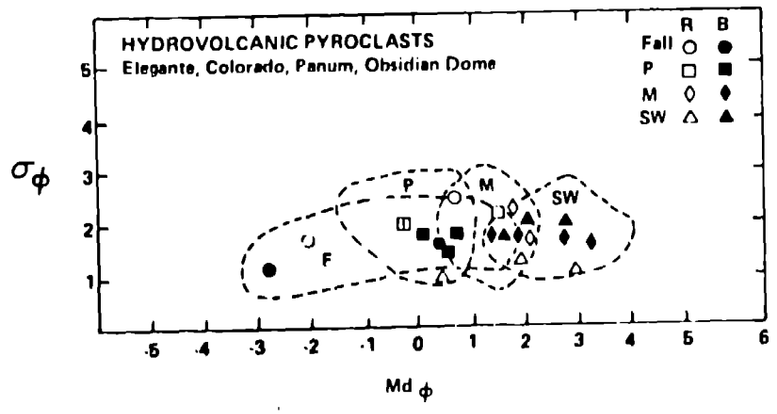
HYDROVOLCANIC PYROCLASTS
Elegante, Colorado, Panum, Obsidian Dome
R B
Fall ○ ●
P □ ■
M ◊ ♦
SW △ ▲
P
M
SW
F
σ_ϕ
Md ϕ

Fig. 1

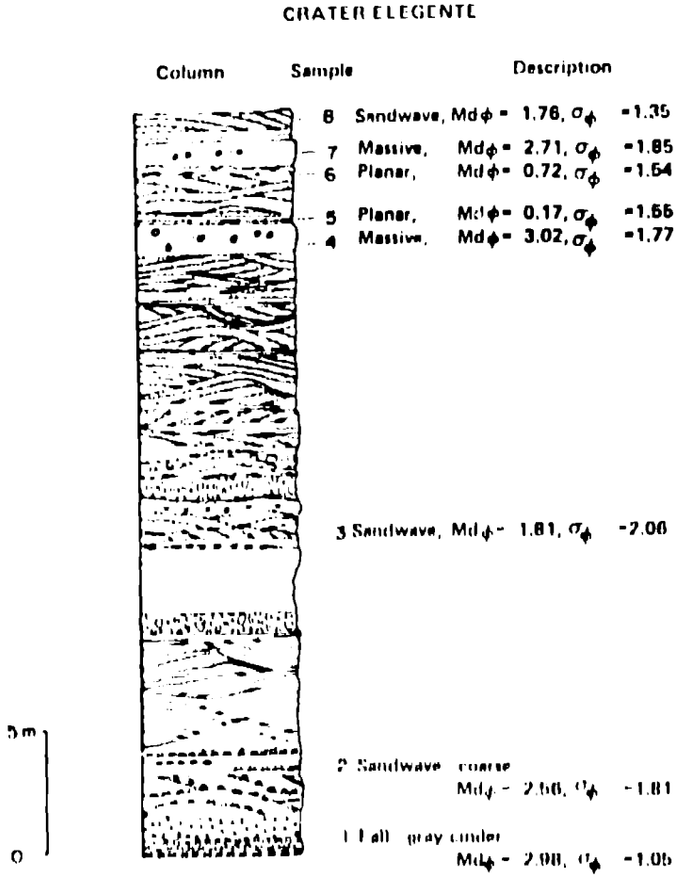
CRATER ELEGENTE
Column
Sample
Description
8 Sandwave, Mdϕ = 1.76, σ_ϕ =1.35
7 Massive, Mdϕ = 2.71, σ_ϕ =1.85
6 Planar, Mdϕ = 0.72, σ_ϕ =1.54
5 Planar, Mdϕ = 0.17, σ_ϕ =1.55
4 Massive, Mdϕ = 3.02, σ_ϕ =1.77
3 Sandwave, Mdϕ = 1.81, σ_ϕ =2.06
5m
0
2 Sandwave coarse
Mdϕ = 2.56, σ_ϕ =1.81
1 Fall gray cinder
Mdϕ = 2.98, σ_ϕ =1.05

Fig. 2

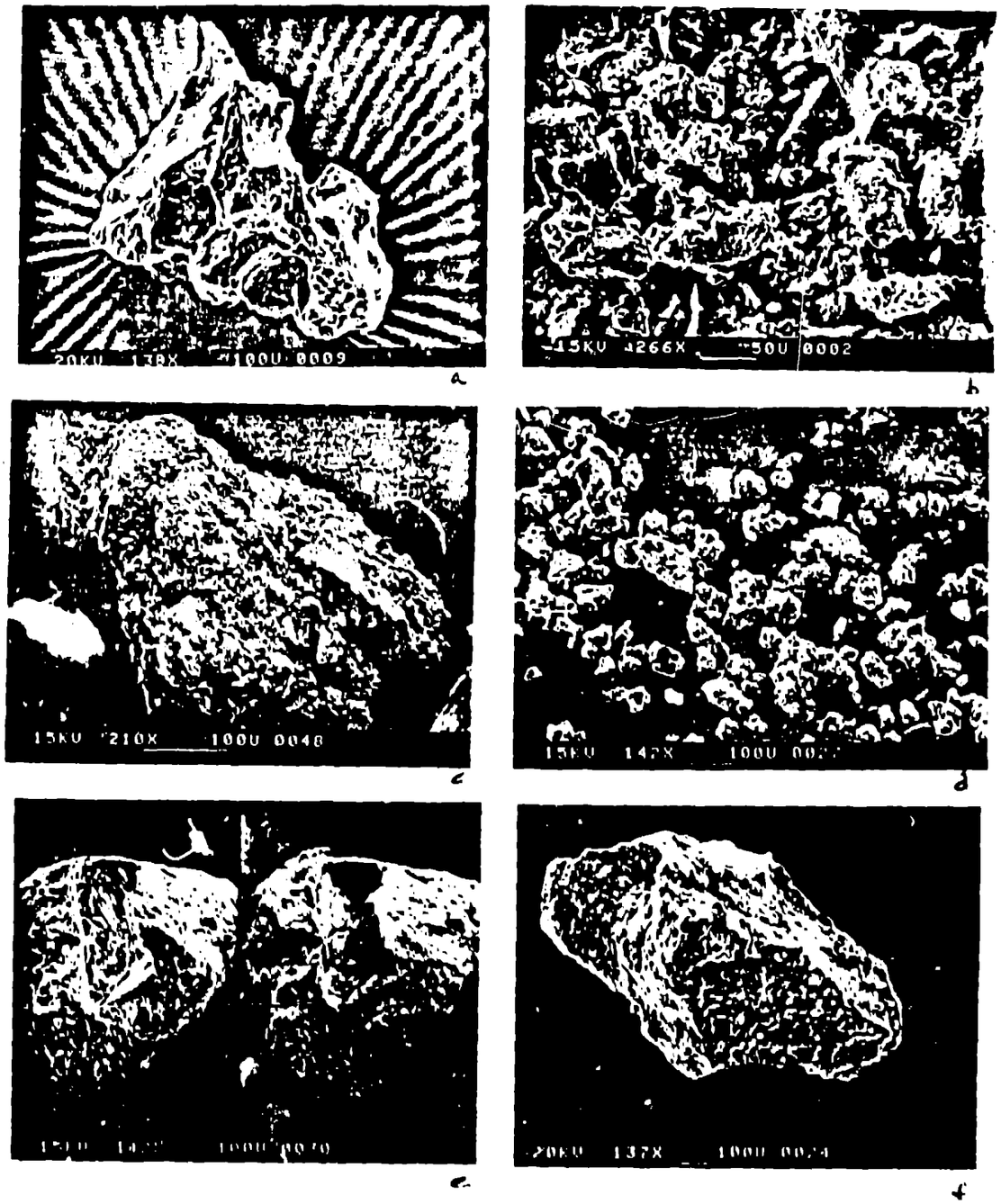
15KV 4266X 50U 0002
15KV 210X 100U 0048
15KV 142X 100U
20KV 137X 100U

Fig 3

CERRO COLORADO

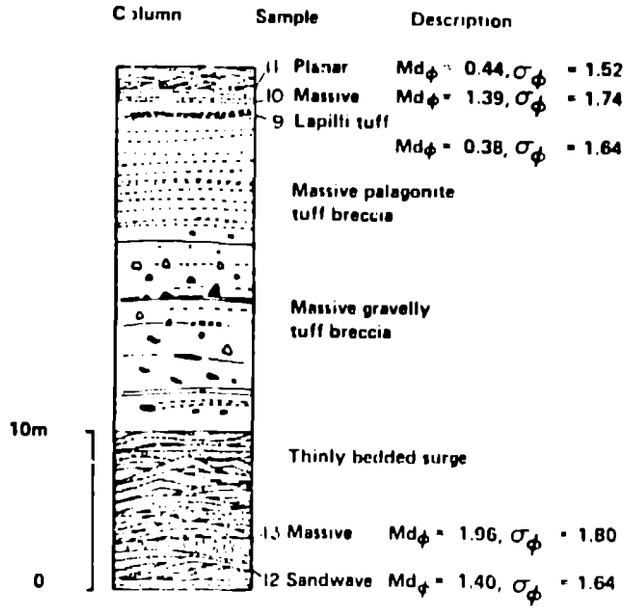

Fig 4

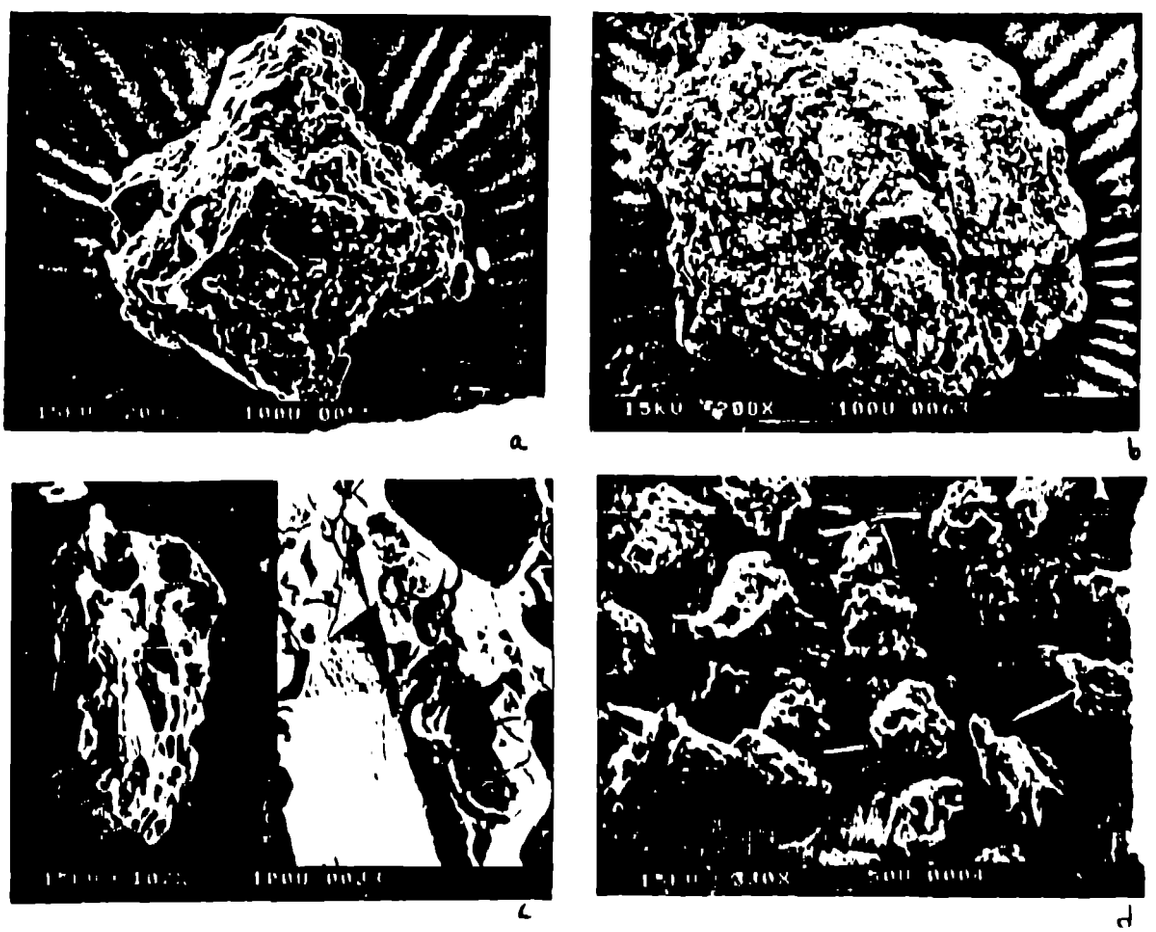

Fig 5

PANUM CRATER

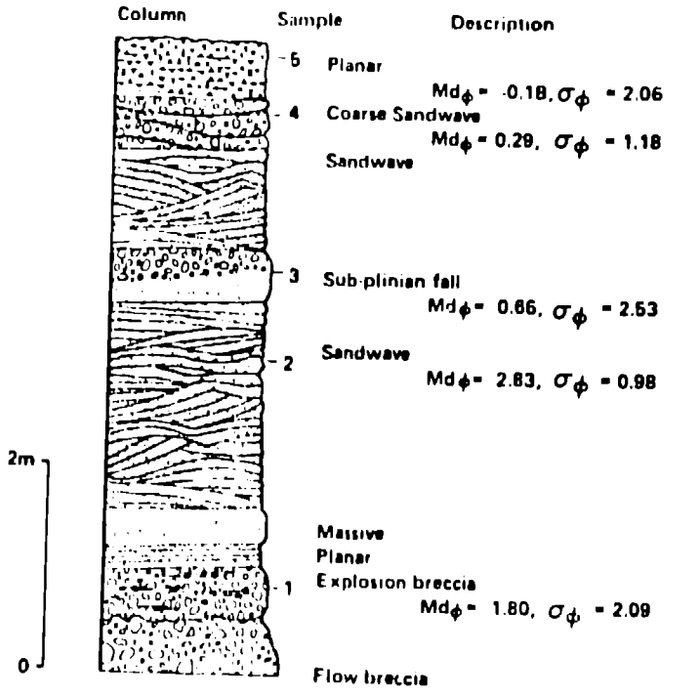

Fig 6

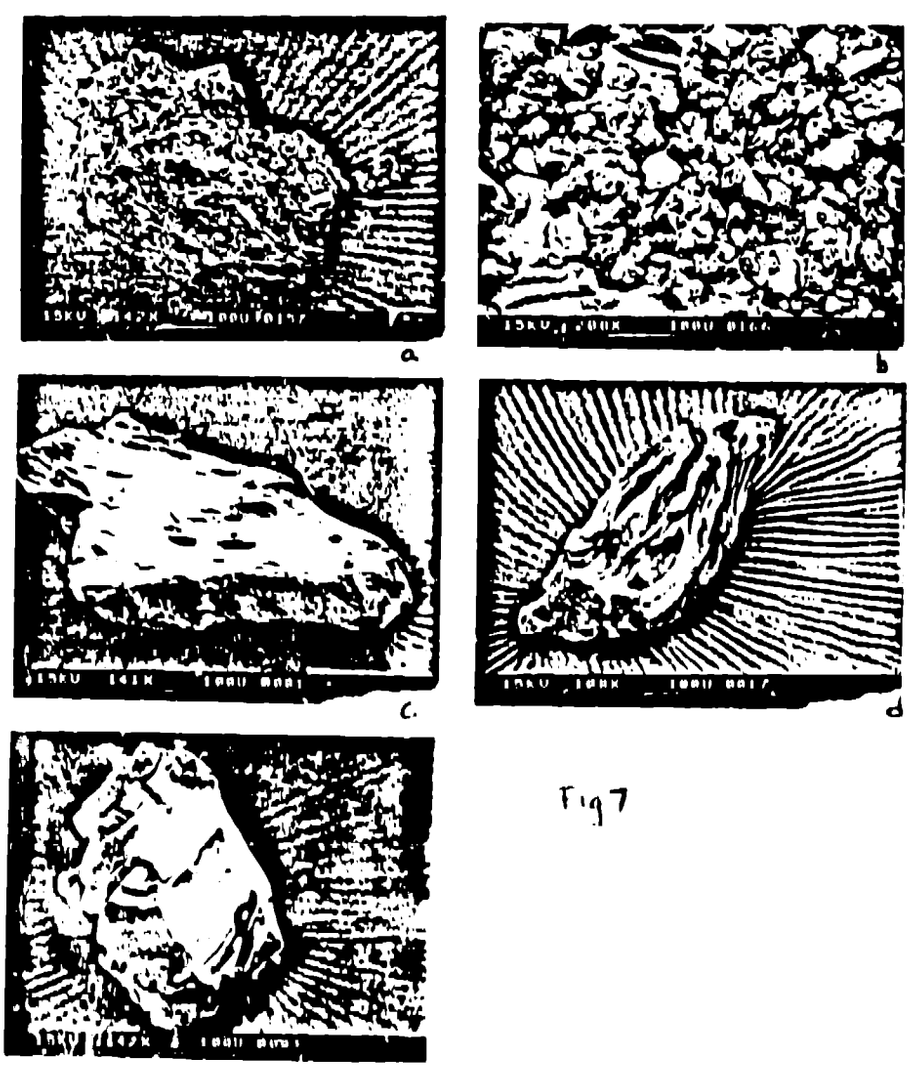

Fig 7

OBSIDIAN DOME

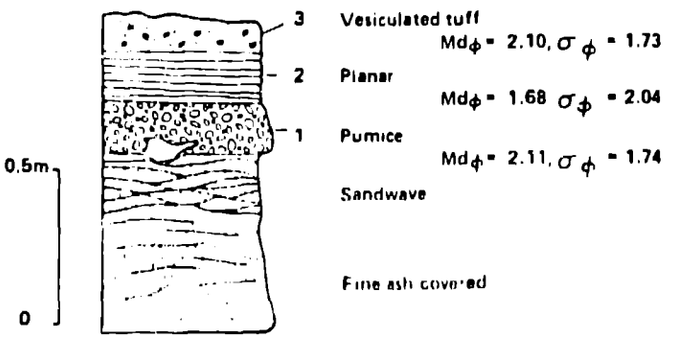

Fig 8

a.

b.

Fig 9.

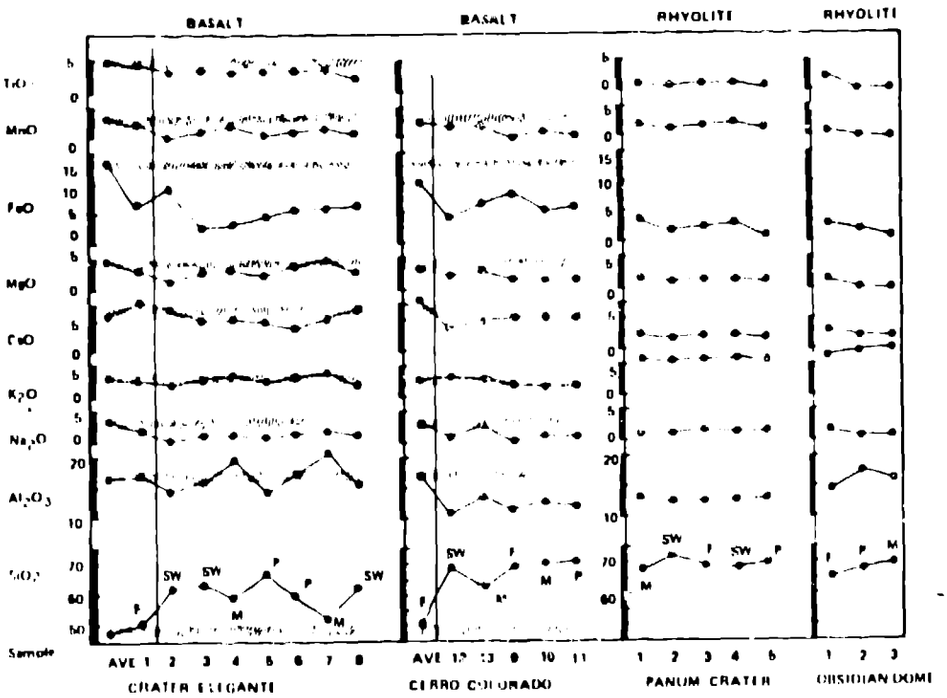
BASALT
BASALT
RHYOLITE
RHYOLITE
TiO2
MnO
FeO
MgO
CaO
K2O
Na2O
Al2O3
SiO2
Sample
AVE 1 2 3 4 5 6 7 8
AVE 12 13 9 10 11
1 2 3 4 5
1 2 3
CRATER ELEGANTE
CERRO COLORADO
PANUM CRATER
OBSIDIAN DOME

Fig. 10

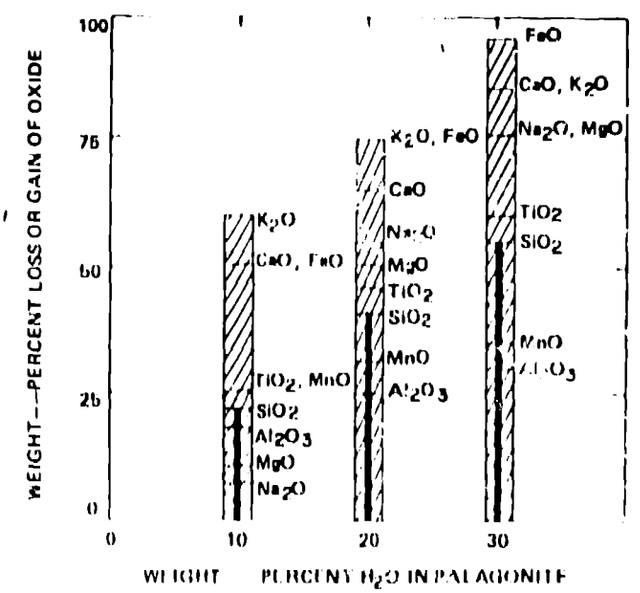
WEIGHT—PERCENT LOSS OR GAIN OF OXIDE
100
75
50
25
0
0
10
20
30
K2O
CaO, FeO
TiO2, MnO
SiO2
Al2O3
MgO
Na2O
K2O, FeO
CaO
Na2O
MgO
TiO2
SiO2
MnO
Al2O3
FeO
CaO, K2O
Na2O, MgO
TiO2
SiO2
MnO
Al2O3
WEIGHT PERCENT H2O IN PALAGONITE

Fig. 11